



Swansea University  
Prifysgol Abertawe



## Cronfa - Swansea University Open Access Repository

---

This is an author produced version of a paper published in:  
*Human Centered Computing: 4th International Conference, HCC 2018, Mérida, Mexico, December, 5–7, 2018, Revised Selected Papers*

Cronfa URL for this paper:

<http://cronfa.swan.ac.uk/Record/cronfa50233>

---

### **Book chapter :**

Mei, J., Shi, H., Chen, D., Li, L., Li, W. & Fan, Q. (n.d). *A Flexible Doubly Clamped Beam Energy Harvester with a Standard Rectifier Electric Circuit*. Yong Tang, Qiaohong Zu, José G. Rodríguez García (Ed.), *Human Centered Computing: 4th International Conference, HCC 2018, Mérida, Mexico, December, 5–7, 2018, Revised Selected Papers*, -78). Springer, Cham.

[http://dx.doi.org/10.1007/978-3-030-15127-0\\_7](http://dx.doi.org/10.1007/978-3-030-15127-0_7)

---

This item is brought to you by Swansea University. Any person downloading material is agreeing to abide by the terms of the repository licence. Copies of full text items may be used or reproduced in any format or medium, without prior permission for personal research or study, educational or non-commercial purposes only. The copyright for any work remains with the original author unless otherwise specified. The full-text must not be sold in any format or medium without the formal permission of the copyright holder.

Permission for multiple reproductions should be obtained from the original author.

Authors are personally responsible for adhering to copyright and publisher restrictions when uploading content to the repository.

<http://www.swansea.ac.uk/library/researchsupport/ris-support/>

# A flexible doubly clamped beam energy harvester with a standard rectifier electric circuit

Jie Mei<sup>1</sup>, Huafeng Shi<sup>1</sup>, Dingfang Chen<sup>1</sup>, Lijie Li<sup>2</sup>, Wenfeng Li<sup>1</sup>, Qiong Fan<sup>1</sup>

(1. Wuhan University of Technology, Wuhan, China, 430063

(2. College of Engineering, Swansea, UK, SA1 8EN)

**Abstract:** While wearable electronics are rapidly developing nowadays, it is greatly limited by the power solutions. Flexible piezoelectric energy harvester presents advantages of high energy density, compact architecture, and easy integration with MEMS, which provides an attractive prospect to power these next generation electronics. Since the flexible devices are usually devised with wavy, island-bridge, and precisely controlled buckling structures, the doubly clamped beam structure for energy harvesting application is analytically studied in this paper. Combine with Euler-Bernoulli beam theory and separation variable method, the analytical expression for output voltage is derived. By conducting the analytical simulation, it is found that the output power is related with the geometry dimensions, external excitation and load resistances. For further validation, experiment is systematically studied. By connecting the standard rectifier electric circuit with the energy harvesting device, it is found that a 0.1 $\mu$ F capacitor can be fully charged in 0.15 s, and the charged output voltage is about 2.5 Volt, which are successfully used for powering LED s.

## 1 Introduction

Since flexible energy harvester provides a prospective solution for powering wearable electronics, remote and mobile environment sensors, and implantable biomedical devices, it has gained more and more attentions during the last decade for advantages of light weight, high flexibility and facile fabrication process. There are several sources that can be converted to electric power, which include mechanical vibration energy, thermal energy and solar energy. Regarding with the mechanical energy conversion process, piezoelectric, triboelectric, electromagnetic and electrostatic energy transducing mechanisms are intensively discussed. Among them, the flexible piezoelectric energy harvester is usually the potential choice for researchers because of its high energy density, compact architecture, straightforward micromachining process and easy integration with MEMS.

In current researches, the cantilever beam with a tip mass is the typical structure for energy harvesting since it can bear large deformation with a lower excited frequency comparing with other geometry structures. However, for flexible energy harvesting device, they are usually fabricated with wavy, island-bridge, and precisely controlled buckling structures to improve the flexibility and stretchability. Therefore, the doubly clamped beam model rather than the cantilever beam structure is selected for analyzing the flexible piezoelectric energy harvester. In 2013, Pillatsch[1] presented a passively self-tuning mechanism of a clamped-clamped beam for wideband energy harvesting utilizing the sliding proof mass. In 2014, Liang[2] connected the doubly clamped beam with rectangular frame to further reduce the resonant frequency using asymmetrical proof mass and supporting mass. In their works, the reduced resonant frequency is 150 Hz and 165 Hz with output power of 0.992mW and 0.844 mW respectively. Zheng conducted an experimental analysis of the

PVDF doubly clamped beam energy harvester and found that its output power is almost twice as large as that of the sandwich beam with vibration frequency being ranged from 1 to 30 Hz at an acceleration of 0.1g[3]. Kashyap[4] derived an analytical model for the doubly clamped unimorph segmented piezoelectric energy harvester with Euler-Bernoulli beam assumptions. In 2016, Emad[5] utilized the stretch strain of the doubly clamped beam structures to harness the ambient vibration energy, in which the geometry structure only composed of piezoelectric material without the elastic substrate. In their simulation results, it showed highly nonlinear phenomena with an output of  $4\mu\text{W}$  from vibration of 0.5g at 70 Hz. In 2018, Damya[6] fabricated a miniature piezoelectric doubly clamped energy harvester with proof mass loading at beams center using MEMS technology, which can output voltage of 4 V and power of  $80\mu\text{W}$  for wireless sensor nodes. Zhou[7] characterized the length effects of piezoelectric layer on the output performance of doubly clamped beam energy harvester under random excitation.

In above studies, the reason for researchers focusing on the doubly clamped energy harvester is because more uniform stress distribution is expected in the clamped-clamped structure comparing with cantilever beam. In order to lower the working frequency, proof masses are attached in all above works. However, the alternative way to reduce the resonant frequency is to utilize the plastic substrate. In this paper, a doubly clamped beam energy harvester with flexible plastic substrate without proof mass is devised. In order to further validate the efficiency, a standard rectifier circuit is connected to power light emitting diodes(LED).

In the paper, the structure is outlined as follows: the analytical model of doubly clamped energy harvester is put forward in section 2. In Section 3, simulation and experimental results are provided to prove the validity of the analytical method. The conclusion remarks are finally made in the section 4.

## 2 Doubly clamped energy harvester model

The schematic figure of the doubly clamped piezoelectric energy harvester is shown as figure 1(a), where one end of the beam is fixed to the frame, and the other end is clamped and excited with applied external force  $P(x, t)$  along the  $x$ -coordinate direction. The harvester is composed of PVDF piezoelectric layer and PVC flexible substrate. The initial length of the energy harvester is  $L$ . When it works, it will be compressed periodically. The corresponding deflection of arbitrary point in the piezoelectric layer is denoted as  $w(x, t)$ . Electrodes are set at the top and bottom surfaces of PVDF material.

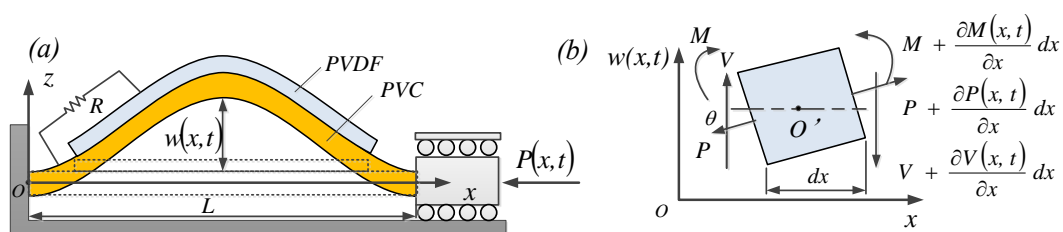


Figure 1 (a) Schematic figure to show the working mechanism of the flexible doubly clamped beam

energy harvester (b) Bending deformation map of finite element in piezoelectric layer

If the doubly clamped beam deformation conforms to the Euler-Bernoulli beam theory, the finite element deformation map of the piezoelectric layer is shown as figure 1 (b). According to the equilibrium equation in transverse direction, formula (1) can be deduced.

$$\rho A(x) dx \frac{\partial^2 w(x, t)}{\partial t^2} = -(V + dV) + V + (P + dP) \sin(\theta + d\theta) - P \sin(\theta) \quad (1)$$

In equation (1),  $\rho$  is the mass density per unit length,  $A(x)$  is the cross-section area,  $V$  denotes the shear force, and  $\theta$  is the rotation angle.

Similarly, according to the moment equilibrium status, equation (2) is deduced as follows,

$$(M + dM) - (V + dV) dx - M = 0 \quad (2)$$

From the relationship between rotation angle and transverse deflection, equation (3) is formulated as,

$$\sin(\theta + d\theta) \approx \theta + d\theta = \theta + \frac{\partial \theta}{\partial x} dx = \frac{\partial w(x, t)}{\partial x} + \frac{\partial^2 w(x, t)}{\partial x^2} dx \quad (3)$$

Combining equations (1)-(3) and ignore the higher order items, it is then derived as equation (4),

$$(EI)_{comp} \frac{\partial^4 w}{\partial x^4} + \rho A \frac{\partial^2 w}{\partial t^2} - P \frac{\partial^2 w}{\partial x^2} = 0 \quad (4)$$

Where  $(EI)_{com}$  denotes the equivalent bending stiffness of the composite beam. It is expressed as (5),

$$(EI)_{com} = \frac{E_c w_c t_c^3 + E_p w_p t_p^3}{12} + \frac{E_c E_p w_c w_p t_c t_p (t_c + t_p)^2}{4(E_c w_c t_c + E_p w_p t_p)} \quad (5)$$

Where  $E_c$ ,  $t_c$ ,  $w_c$  are Young's modulus, thickness and width of substrate respectively.

If utilizing the separation variable method, the transverse displacement  $w(x, t)$  can be assumed as (6),

$$w(x, t) = W(x) (A \cos \omega t + B \sin \omega t) \quad (6)$$

By substituting equation (6) into (4), the following equation is obtained,

$$(EI)_{comp} \frac{d^4 W}{dx^4} - P \frac{d^2 W}{dx^2} - \rho A \omega^2 W = 0 \quad (7)$$

Then the general form of solution to equation (7) is derived as (8),

$$W(x) = A \cosh sx + B \sinh sx + C \cos sx + D \sin sx \quad (8)$$

In equation (8), A, B, C and D are constants. Combining with boundary conditions of the doubly clamped beam energy harvester,  $\sinh sl \sin sl = 0$ , the mode shape function is derived as (9),

$$W(x) = \sin\left(\frac{n\pi}{l}x\right) \quad n = 1, 2, 3, \dots \quad (9)$$

And the nature frequency is calculated as equation (10),

$$\omega_n = \frac{\pi^2}{l^2} \sqrt{\frac{(EI)_{comp}}{\rho A}} \sqrt{n^4 - \frac{n^2 F_0 l}{\pi^2 (EI)_{comp}}} \quad (10)$$

In order to solve the forced vibration of doubly clamped beams, separation variable method is utilized as equation (11),

$$w(x, t) = \sum_{n=1}^{\infty} W_n(x) q_n(t) \quad (11)$$

Where  $W_n(x)$  denotes the mode shape at nth natural frequency, and  $q_n(t)$  represents the corresponding generalized coordinate.

If (11) is substituted into equation (4), then (4) can be rewritten as (12),

$$(EI)_{comp} \left( \sum_{n=1}^{\infty} \frac{d^4 W_n(x)}{dx^4} q_n(t) \right) + \rho A \sum_{n=1}^{\infty} W_n(x) \frac{d^2 q_n(t)}{dt^2} = P(x, t) \frac{d^2 W_n(x)}{dx^2} q_n(t) \quad (12)$$

Through integrating above equation from 0 to 1, it can be simplified into the following form with orthogonality conditions.

$$\frac{d^2 q_n(t)}{dt^2} + \omega_n^2 q_n(t) = \frac{1}{\rho A b} Q_n(t) \quad (13)$$

Where  $Q_n(t) = \int_0^l P(x, t) W_n(x) dx$ , and  $b = \int_0^l W_n^2(x) dx$ .

Then the solution to equation (13) is obtained as (14).

$$q_n(t) = A_n \cos \omega_n t + B_n \sin \omega_n t + \frac{1}{\rho A b \omega_n} \int_0^t Q_n(\tau) \sin \omega_n(t - \tau) d\tau \quad (14)$$

In (14), the first two terms represent the vibration state under transient conditions, and the third term represents the vibration state under steady state. Therefore, when solving the dynamic model, equation (14) can be simplified to (15).

$$q_n(t) = \frac{1}{\rho A b \omega_n} \int_0^t Q_n(\tau) \sin \omega_n(t - \tau) d\tau \quad (15)$$

Combining equations (9) and (15), the deflection can be derived as (16),

$$w(x, t) = \frac{2F_0}{\rho A l} \sum_{n=1}^{\infty} \frac{1}{\omega_n^2 - \omega_0^2} \sin \frac{n\pi}{2} \sin \frac{n\pi x}{l} \sin \omega_0 t \quad (16)$$

Then the stress of an arbitrary point on the beam can be expressed as (17),

$$\sigma(x, t) = E_p y' \frac{\partial^2 w(x, t)}{\partial x^2} \quad (17)$$

Where  $E_p$  is the elastic modulus of piezoelectric material.

Substituting the formula (16) into (17), the deflection can be rewritten as (18),

$$\sigma(x, t) = -\frac{2F_0 E_p y'}{\rho A l} \sum_{n=1}^{\infty} \frac{1}{\omega_n^2 - \omega_0^2} \left( \frac{n\pi}{l} \right)^2 \sin \frac{n\pi}{2} \sin \frac{n\pi x}{l} \sin \omega_0 t \quad (18)$$

Because the piezoelectric vibrator is operating at low frequency, it suggests that  $\omega_n \gg \omega_0$ . Then

(18) can be rearranged as (19),

$$\sigma(x, t) = -\frac{2F_0 E_p y'}{\rho A l} \sum_{n=1}^{\infty} \frac{1}{\omega_n^2} \left( \frac{n\pi}{l} \right)^2 \sin \frac{n\pi}{2} \sin \frac{n\pi x}{l} \sin \omega_0 t \quad (19)$$

Substituting the above formula into the piezoelectric constitutive equation  $D_3 = d_{31} T_1 + \varepsilon_{33}^T E_3$ , the electric displacement is obtained as (20),

$$D_3(x, t) = -\frac{2d_{31} F_0 E_p y'}{\rho A l} \sum_{n=1}^{\infty} \frac{1}{\omega_n^2} \left( \frac{n\pi}{l} \right)^2 \sin \frac{n\pi}{2} \sin \frac{n\pi x}{l} \sin \omega_0 t + \varepsilon_{33}^T E_3 \quad (20)$$

By integrating (20) across the electrode surface area, the generated charge can be deduced as (21),

$$Q_3 = \frac{2\pi w_p d_{31} F_0 E_p y'}{\rho A l^2} \sum_{n=1}^{\infty} \frac{n}{\omega_n^2} \left[ \cos \frac{n\pi a}{l} - \cos \frac{n\pi(a+l_p)}{l} \right] \sin \frac{n\pi}{2} \sin \omega_0 t + \frac{w_p l_p \varepsilon_{33}^T}{t_p} V_3(t) \quad (21)$$

Where  $y'$  represents the distance from an arbitrary point to the neutral plane,  $l$  and  $l_p$  are lengths of the substrate and piezoelectric material respectively.  $a$  is the distance from the piezoelectric material to the length boundary.  $w_p$  denotes the width of piezoelectric layer.

Then current formula can be derived by integration of (21) with respect to time.

$$I = \frac{dQ(t)}{dt} = \frac{2\omega_0 \pi w_p d_{31} F_0 E_p y'}{\rho A l^2} \sum_{n=1}^{\infty} \frac{n}{\omega_n^2} \left[ \cos \frac{n\pi a}{l} - \cos \frac{n\pi(a+l_p)}{l} \right] \sin \frac{n\pi}{2} \cos \omega_0 t + C_p \frac{dV(t)}{dt} \quad (22)$$

Where  $C_p = \frac{w_p l_p \varepsilon_{33}^T}{t_p}$ , and  $t_p$  is the thickness of piezoelectric layer.

Combining equation (21) and (22), the induced potential can be obtained as (23),

$$V(t) = \frac{2\pi w_p d_{31} F_0 \omega_0 E_p y'}{\rho A l^2 \sqrt{C_p^2 + \frac{1}{R_L^2}}} \sum_{n=1}^{\infty} \frac{n}{\omega_n^2} \left[ \cos \frac{n\pi a}{l} - \cos \frac{n\pi(a+l_p)}{l} \right] \sin \frac{n\pi}{2} \sin(\omega_0 t + \phi) \quad (23)$$

Since high-order vibration modes hardly impact the induced voltage, for the convenience of calculation, only the fundamental mode term is considered in the output equation. Then (23) is rewritten as (24),

$$V_o(t) = \frac{2w_p l^2 d_{31} F_0 \omega_0 E_p y'}{\pi^3 (EI)_{comp} \sqrt{C_p^2 + \frac{I}{R_L^2} \left( I - \frac{F_0 l}{\pi^2 (EI)_{comp}} \right)}} \left[ \cos \frac{\pi a}{l} - \cos \frac{\pi(a + l_p)}{l} \right] \sin \omega_0 t \quad (24)$$

From equation (25), it can be deduced that the output potential is determined by the geometry dimensions, external excited force and load resistance.

### 3. Simulation and Experiment results

In order to prove the feasibility of the model, both analytical analysis and experimental characterization are conducted. Table 1 shows the parameters of the doubly clamped energy harvester. Assuming that the externally applied load  $F_0$  is 3N, and the excited frequency is 30 Hz. From equation (24), the varying trend of deduced output voltage and output power versus time are shown as figure 2(a) and (b) respectively, where the connected load resistance is 5MΩ. In the simulation results, the amplitude of output voltage is around 3.67 Volt, and the instantaneous power output is 2.7 μWatt.

Table 1 parameters for the doubly clamped energy harvester

l	lp	a	wc	wp	tc
30 mm	20 mm	5 mm	10 mm	10 mm	3 mm
tp	Ec	Ep	d31	ε <sub>33</sub>	
2 mm	2900 MPa	3900 MPa	21 pc/N	12 F/m	

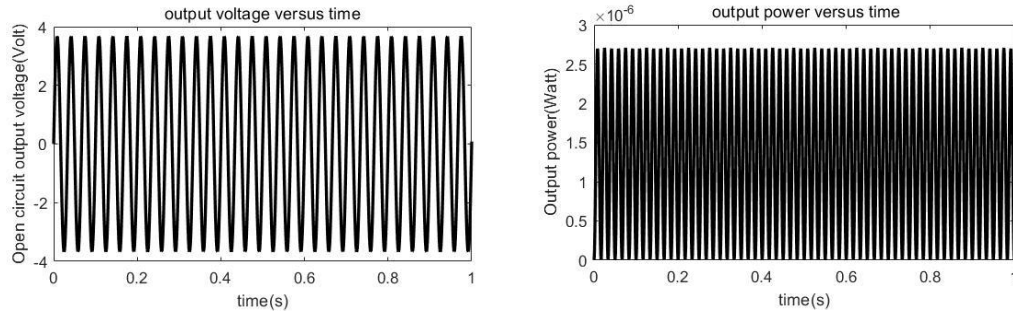


Figure 2 Simulation results of output voltage and power by utilizing the analytical model

For further study of doubly clamped energy harvester model, the prototype has been fabricated. Figure 3(a) shows the experiment setup which include devices of the computer interface, signal generator (AFG3021C), power amplifier, vibrating shaker (Modal 50A Vibration Exciter), standard AC-DC rectifier circuit and the data acquisition card. Figure 3(b) is the enlarged view of the prototype.

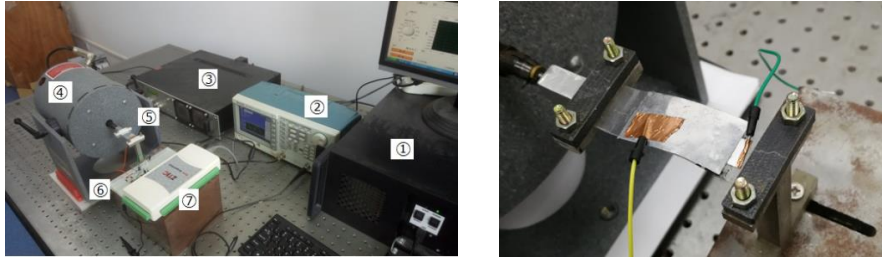


Figure 3 (a) Experimental setup, in which ① is the computer, ② is the signal generator, ③ is power amplifier, ④ is vibrating shaker, ⑤ is the doubly clamped energy harvester, ⑥ is the AC-DC rectifier circuit and ⑦ is data acquisition card; (b) is the enlarged view of the energy harvesting device.

From figure 3(b), it is observed that the flexible energy harvester is doubly clamped. When the shaker is excited by the signal generator, it will move one end of the device sinusoidally along the axial direction, while the other end is kept fixed. Since both the piezoelectric patch and the substrate are both polymers, the device is easily deformed into curve structure. As the piezoelectric layer is strained, the mechanical energy will be converted into electric energy through the direct piezoelectric effect. Figure 4 shows the result of the output voltage that have been captured by the data acquisition card. From the results, it shows that the amplitude of the output voltage is around 3 Volt, and the resonant frequency is 30 Hz, which agrees well with the analytical results.

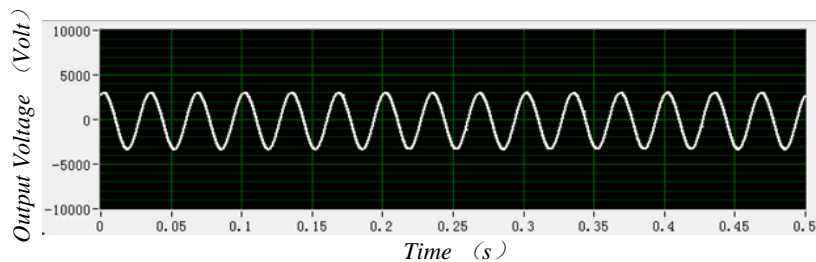


Figure 4 Waveform captured by the data acquisition card

Figure 5(a) shows the varying trend of output voltage with respect to the excited frequency. As the excited frequency is changed from 0.5 Hz to 100 Hz with a load resistance of 3 MΩ, the output voltage is increased rapidly in range (0.5Hz, 30Hz). When it climbed up to 30Hz, the reached the maximum output of 2.35Volt. When it continued increasing the excited frequency, the induced voltage will be decreased. The same varying trend is observed when external load resistance is changed to be 4 MΩ and 5 MΩ. Figure 5(b) depicts the relationship between output power and external load resistance. From the trendline, a peak value of 4.8 μW is found, where the optimum load resistance of 3 MΩ is determined.



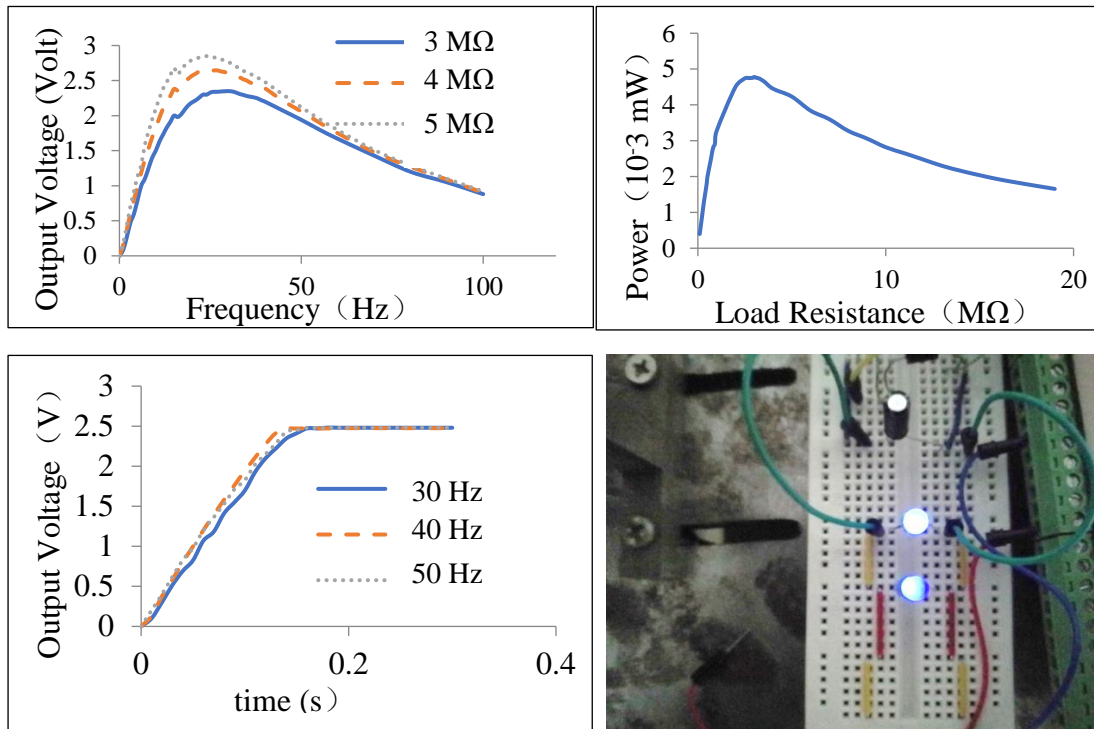


Figure 5 (a) DC Output voltage versus frequency; (b) output power versus load resistance; and (c) output voltage in the charging process through standard rectifier electric circuit ; and (d) applications of the energy harvester to power LEDs.

Although the output voltage across the electrodes are alternative signals, it can be rectified into DC signal through the standard bridge circuit. Figure 5(c) represents charging process of capacitor by the flexible energy harvester under different excitation frequency, where the capacitance is 0.1 $\mu$ F. From the results, it is observed that the capacitor can be fully charged in 0.15s, and the charging speed is independent with the excited frequency. Since the rectified output voltage in the standard AC-DC circuit is about 2.5 Volt, it can be utilized to power electronics. Figure 5(d) shows the possibility of the flexible doubly clamped energy harvester to power LEDs, which can make the flexible doubly clamped energy harvester present more attractive prospects in the future.

#### 4. Conclusion

In the paper, the analytical model of the flexible energy harvester is provided based on the Euler-Beam theory and separation variable method. In order to prove the feasibility of the model, both simulation and experimental analysis are provided. Through comparison, the simulation results of 3.67 Volt and instantaneous power 2.7  $\mu$ Watt coincides well with experiments. For further study of doubly clamped energy harvester model, the authors have also fabricated the prototype. By connecting the device with a standard AC-DC rectifier electric circuit, the 0.1 $\mu$ F capacitor can be fully charged up to 2.5 Volt in 0.15 s, through which LEDs is lit to show its attractive prospects.

## **Acknowledgment**

This paper was supported by the Natural Science Foundation of Hubei Province (20181j001: Interfacial Defects Initiation Mechanism of Flexible Laminated Thin Film Energy Harvester and its Fabrication Process) and the open fund of Jiangxi Province Key Laboratory of precision drive & control (PLPDC-KFKT-201604).

## **Reference**

- [1] Pillatsch P, Miller L M, Halvorsen E, et al. Self-tuning behavior of a clamped-clamped beam with sliding proof mass for broadband energy harvesting[C]// Journal of Physics: Conference Series, Volume 476, PowerMEMS 2013 conference, 2013:2068.
- [2] Zhu Liang, Xu Chundong, Ren Bo, et al. A low frequency and broadband piezoelectric energy harvester using asymmetrically serially connected double clamped-clamped beams[J]. Japanese Journal of Applied Physics 53, 087101(2014).
- [3] Zheng Y, Wu X, Parmar M, et al. Note: High-efficiency energy harvester using double-clamped piezoelectric beams[J]. Review of Scientific Instruments, 2014, 85(2):102.
- [4] Kashyap R, Lenka T R, Baishya S. A Model for Doubly Clamped Piezoelectric Energy Harvesters With Segmented Electrodes[J]. IEEE Electron Device Letters, 2015, 36(12):1369-1372.
- [5] Emad A, Mahmoud M A E, Ghoneima M, et al. Modeling and analysis of stretching strain in clamped-clamped beams for energy harvesting[C]// IEEE, International Midwest Symposium on Circuits and Systems. IEEE, 2017:1-4.
- [6] Damya A, Sani E A, Rezazadeh G. An innovative piezoelectric energy harvester using clamped-clamped beam with proof mass for WSN applications[J]. Microsystem Technologies, 2018(2017):1-9.
- [7] Zhou X, Gao S, Jin L, et al. Effects of changing PZT length on the performance of doubly-clamped piezoelectric energy harvester with different beam shapes under stochastic excitation[J]. Microsystem Technologies, 2018(11):1-15.